SCALE OF MISSING INFORMATION: USING A SKYLER II PHASED ARRAY RADAR TO SHOW THE MAGNITUDE AND SCALE OF ATMOSPHERIC PHENOMENA BELOW NEXRAD RESOLUTION

Theodore Mackey

Dr. Stephen Guimond

Hampton University, Hampton, VA

Department of Atmospheric and Planetary Sciences and Severe Weather Research Center

ABSTRACT

In the US, real-time weather warnings for precipitation and extreme winds are driven by radar observations, namely data from the National Weather Service (NWS) NEXRAD Radar System. These instruments cover the vast spatial extent of the country but have temporal and spatial resolutions that make them poor for observing small-scale turbulent features, especially in extreme weather events, such as hurricanes and tornadoes. As extreme weather events become more common and more powerful, understanding the characteristics of small-scale turbulent features is vital for both human health and the forecasting of such systems. By calibrating and utilizing a Skyler II radar system, which has an order of magnitude higher spatial and temporal resolution, we found that the information in features smaller than 2-3 km is being under-represented by the current NEXRAD instruments. On one of our two case days, November 11th, 2024, Skyler reported 4 times the energy NEXRAD reported from features that have spatial scales of 1 - 3 km. This feeds into various products developed from radar measurements, such as rainfall rates, water mass change, and even tornado detection.

INTRODUCTION

Most of the damaging weather that occurs on Earth is driven by movements of water. As water is moved vertically in the atmosphere, it condenses into clouds, which can produce flooding rains. This condensation process also releases energy into the atmosphere through latent heat release, which can lead to increased wind speeds, increased condensation, and lead to storm formation and intensification. Being able to observe the movement of water parcels in the atmosphere is thus vital for human safety, as these storms cause damage to both life and property. As a result, forecasting when and where extreme weather will occur, as well as the precipitation and winds that accompany such events, has been a key part of research and study. To observe water movements in the atmosphere radar systems have been deployed in the US since 1942 to observe water movements in the atmosphere.

Radar (Radio Detection and Ranging) is a remote sensing technology that operates using electromagnetic radiation, usually emitting in the microwave regime between 0.2 - 300 GHz for weather measurements. Radar technology was originally developed and designed for military purposes, but it was found that what the military considered noise was information about atmospheric phenomena (1). Radar systems emit rapid pulses of light from the radar dish face and then detect the number of returning photons and their phase compared to the emitted photons.
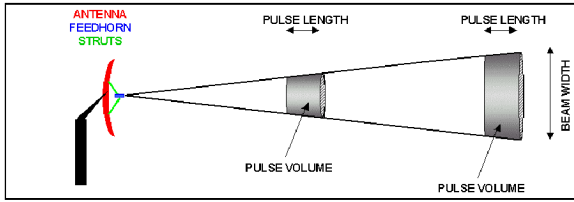
Figure 1. Dramatization of radar beam expansion after pulse emission. Credit to UCAR for this cartoon

As the emitted volume moves away from the dish, it expands in both azimuthal and elevation directions, while the radial distance stays constant. Any data collected in that volume is averaged, so as the pulse moves further from the dish, the data values returned are averaged over a larger spatial extent. This can result in poor data precision far away from the radar.

The number of returned photons is represented by Radar Reflectivity, which is reported in dBz units and is calculated using the following equation:

$$R_{dBz} = 10 * log_{10}(R_Z) \qquad (1)$$

Here, R_Z is the number of photons that returned to the detector. By comparing the phase of the emitted and returned photons, the radial velocity can also be computed. This velocity is a combination of the three components of the wind, N/S (U wind), E/W (V wind), and vertical (W wind), and is related to those wind components by the following equations:

$$V_r = \frac{(UX+VY+WZ)}{\sqrt{X^2+Y^2+Z^2}} \qquad (2)$$

By changing the direction of emission, either mechanically (rotating a dish) or electronically (steering the beam emission from the face of the radar), a radar system can map out atmospheric phenomena in the atmosphere.

In the United States, the National Weather Service operates 159 Next-Generation Radar (NEXRAD) Weather Surveillance Radars (WSR) across the Continental US and overseas. These systems are labeled WSR-88D radars, which mechanically steer a large dish in a continuous circular pattern, operating at 2700-3000 MHz, or around 10 cm (2). These systems are impressive, covering nearly the entire Continental US above at 3 km, with a few gaps in the Mountainous West (3). These systems report Radar Reflectivity covering 2 km to 460 km from their dish and can report data from near the surface up to 150 km if necessary by changing the elevation angle of their dish as it rotates between $\sim 0.4^0$-19.5^0. NEXRAD systems operate with an azimuthal spacing of 0.5^0-1^0, depending on the current scan parameters. Their spatial resolution is 250m, and their temporal resolution is ~4-6 minutes. Data from a NEXRAD system is reported over a full volume, a set of 360^0 scans over each of the elevation angles. However, water based weather occurs completely mainly in the troposphere, which signifies all air from the surface to around 15 km altitude. Furthermore, the most important information for issuing warnings to nearby population centers is the near surface rain patterns. Due to this, each NEXRAD system performs multiple low elevation angle scans in the process of completing a full volume while only performing one scan at the elevation angles large elevation angles. As an example, NEXRAD KAKQ (KAKQ) was used in this study, and it visits the 11 elevation angles greater than 2.5^0 once, while three elevation angles below 2.5^0 are visited at least twice. KAKQ visits the lowest angle, 0.48^0 elevation, 4-6 times per volume scan, resulting in a temporal resolution ~2 minutes. This system

was chosen due to its proximity to Hampton, located in Wakefield, VA, 60 km West of Hampton University.

Even with this temporal resolution, there are still atmospheric phenomena that occur at temporal and spatial scales below the ability of NEXRAD to observe. To combat the blindness to small-scale phenomena, Phased Array Radars (PARs) have been adapted and utilized for weather purposes. Prior work on the application of PARs showed their ability to both observe at shorter temporal and spatial scales, as well as be more steerable to objects of interest (4 and 5). The lack of high temporal resolution data in extreme weather events is also being investigated from satellite remote sensing, including the upcoming NASA INCUS mission (6).

Located at Hampton University, the Raytheon Skyler II Phased Array (Skyler) allows for such an investigation to occur over the Hampton Roads Area.

Figure 2. The Skyler II Phased Array Radar (mid left) is located on top of the Harbor Center at Hampton University. Also pictured is the Hampton University Direct Broadcast Satellite (DBS) (lower right)

A more detailed explanation of the Skyler system can be found in the literature (7 and 8). These systems electronically steer their emission, while NEXRAD mechanically rotates a dish to steer emission. As Skyler can capture information more rapidly, we are now able to resolve small-scale turbulence for the first time.

In this work our main focus is using spectral analysis techniques on Radar Reflectivity Returns from both KAKQ and Skyler to show the magnitude of information missing from KAKQ returns. As part of this computation, we discuss the calibration of Skyler to KAKQ and show the difference in computed rainfall rates from the two systems.

METHODS

This project was split into three parts, each of which was built upon the previous. We focus solely on Radar Reflectivity here, as we lack another system to allow us to compute the true wind field. One of our current areas of interest is how to compute a wind field in the Hampton Roads area, either through a modeling or an instrumentation approach. Our

	KAKQ	Skyler
Operational Wavelength	10 cm	2 cm
Spatial Resolution	250 m	24 m
Temporal Resolution	~3-6 minutes	30 seconds
Operational Range	460 km	30 km
Azimuthal Range	360^0	90^0
Elevation Spacing	Varies	2^0
Azimuthal Spacing	0.5^0 -1^0	0.64^0

Table 1. NEXRAD KAKQ and
Skyler II Operational Parameters

initial step was to compute a calibration bias for Skyler, using KAKQ as the truth reflectivity. Our process for computing this is discussed in the Appendix. The set of spatial and temporal matched KAKQ and Skyler volume scans is necessary for this analysis to ensure that we are inputting the same features viewed from the two systems into our computations.

Spectral Analysis

To perform spectral analysis, we use the raw Skyler and KAKQ data that we matched temporally during our bias computation. We add our computed bias to the Skyler Radar Reflectivity before we interpolate the datasets to the same fixed grid, a cube 25m x 25m x 25m covering 30 km East, 24 km South, and 20 km North of Skyler, from the surface up to 5 km. This cube was chosen to help reduce computing time while focusing on low-altitude data, as turbulent features often occur due to the air-ground interaction. However, this cube does not represent the actual ability of each instrument to observe the atmosphere. Thus, after our interpolation we smooth each dataset to the instrument's observational capability. For Fourier Analysis, this value is twice the observational spacing: 500 m for KAKQ and 50 m for Skyler. Since Skyler is pointed directly East, we compute a Fast Fourier Transform (FFT) along a single Eastward position. For each matchup, we find sections of North/South values that contain no NaN values, allowing for the FFT to be computed along the longest possible distance. This transform is computed on as many vertical planes as possible and then averaged. This process is repeated for three separate days, and then all the resulting FFT outputs are averaged and reported.

Rainfall Rates

While the FFT computation allows us to see the magnitude of missing information, we sought to add a real-world example to drive home the difference that this missing information can have. For this purpose, we have computed the rainfall rate using the NWS relationship between rainfall rate (R, [mm/hr]) and the raw reflectivity (Z [unitless]) (9):

$$Z = 300R^{1.4} \qquad (3)$$

This rate is computed both over 2D slices at set altitude, and then the spectra of this rainfall rate profile is computed in the same manner as the radar reflectivity profile. To discuss the accuracy of our profiles, we plan to use a disdrometer and tipping rain gauge bucket located on Island 3 of the Chesapeake Bay Bridge-Tunnel (CBBT) (10) to validate our rainfall rate computations.

Since the disdrometer and rain gauge are surface point measurements, correlating the exact value from Skyler to a ground value is difficult for two main reasons:

(1) The CBBT is located nearly 25 km East of Skyler. At that distance, the emitted pulse volume covers a volume 25 m x 700 m x 925 m. Since the radar system averages over this height, we cannot tell the distribution of rain drop scatters, and thus the value at the surface is unobtainable from the radar

(2) We do not currently have a way to compute the fall speed of the droplets, as we cannot yet obtain a 3D wind field. Thus, we cannot be sure when or where the rainfall we are computing from Skyler lands at the surface.

However, we can plan to expand more on this in our future work.
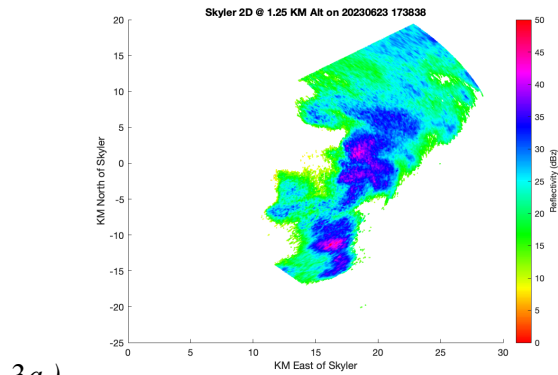
3a.)
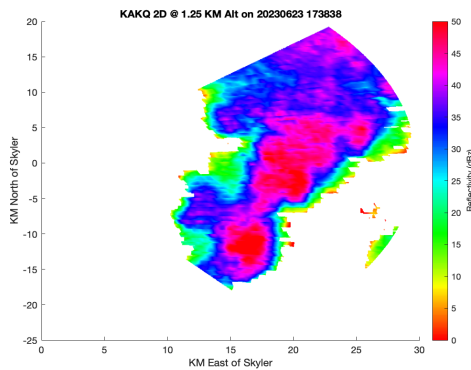
3b.)
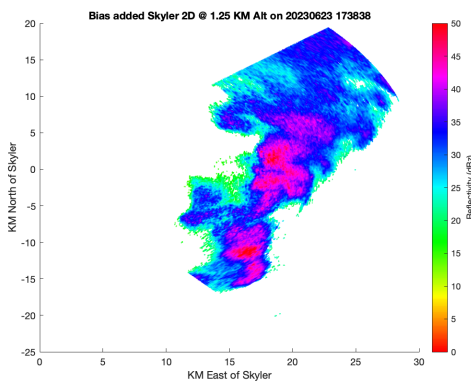
3c.)

Figure 3. Interpolated Radar Reflectivity Spectra from raw Skyler (a), KAKQ (b), and bias-added Skyler (c) on June 23rd, 2023. These cross sections are at 1.25 km altitude and show the effects of Skyler's higher spatial sampling resolution in the horizontal.

RESULTS

From our calibration computation, detailed in the Appendix, we found that Skyler has a mean bias of 7.07 ± 3.51 dBz, which we apply to Skyler for all of our future calculations, as shown in Figure (2).
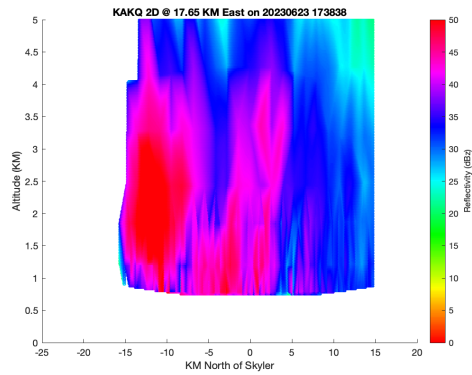
4a.)
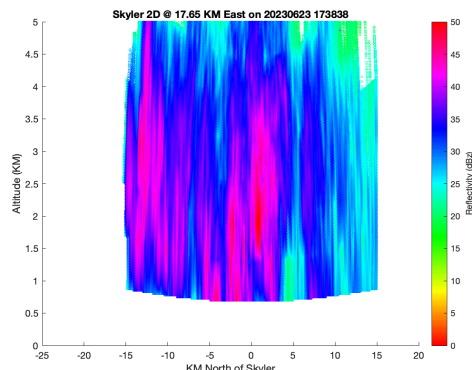
4b.)

Figure 4. Interpolated Radar Reflectivity Spectra from bias-added Skyler (a) and KAKQ (b) on June 23rd, 2023. These cross-sections are at 17.65 km East of Skyler and show the effects of Skyler's higher spatial sampling resolution in the vertical.

Our spectral analysis work resulted in two key findings:

(1) Skyler can resolve features below KAKQ's ability to observe. This was the expected result as KAKQ cannot physically resolve features below 500 m, as it observes the atmosphere at a spatial resolution of 250 m. The horizontal cross-sections in Figure 2 demonstrate this.

(2) KAKQ spectral resolution falls off much faster than we expected, with large differences in reported energy appearing at scales smaller than 1-3 km, which is the regime of turbulence that we are trying to understand.

5a.)
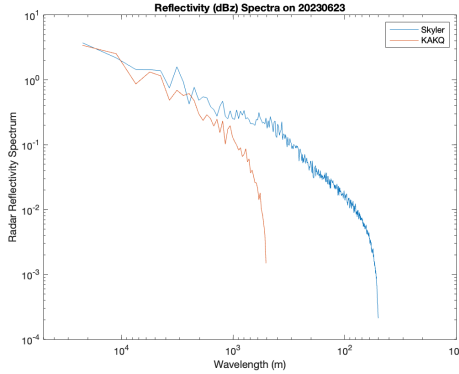
5b.)
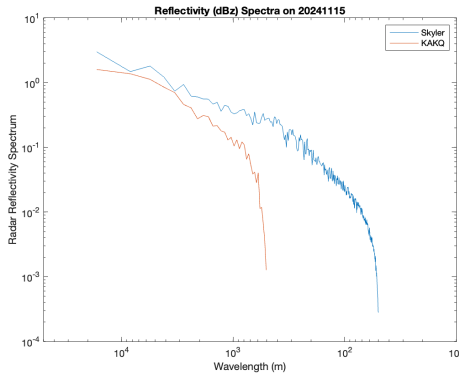
Figure 5. Radar Reflectivity Spectra for Skyler and KAKQ computed on June 23rd, 2023 (a), November 15th, 2024 (b). These plots are averaged over 5 and 15 minutes, respectively. In (a), the energy difference between KAKQ and Skyler becomes noticeable at scales of 2 km, with the difference remaining a factor of 2 until 1 km, where it rapidly falls off for smaller scale features, until the difference is a factor of 4 for 750 m features. This fall-off occurs earlier in (b), where a factor of 2 difference becomes noticeable at scales of 3 km, and a factor of 4 difference is visible at scales as large as 1 km.

From these spectra, Skyler can report <u>four times</u> the information about the spatial variation of radar reflectivity across all feature scales compared to KAKQ. This was also computed for rainfall rates, showing that Skyler reports <u>twice</u> the information about the spatial variation of rainfall.

6a.)
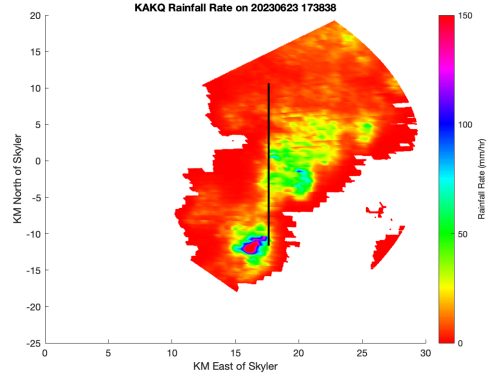
6b.)
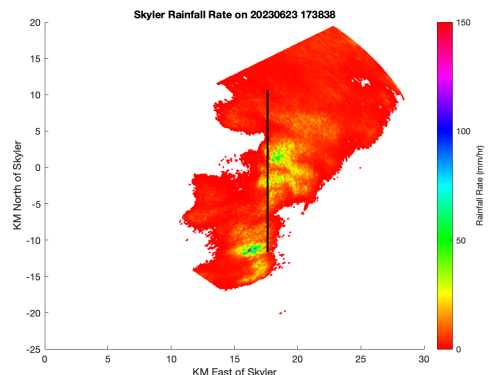
6c.)
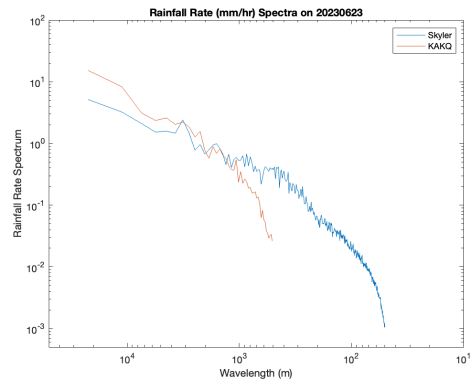
Figure 6. Plots (a) and (b) are vertical cross sections at 1.25 KM Altitude on June 23rd, 2023, for Nexrad and Skyler, respectively. The vertical black line indicates the location and length of our spectral computation. Returns from Skyler show more variability in the structures, as shown in (c)

DISCUSSION

From this work, we support that small-scale turbulent motions that are unobservable to the current NWS NEXRAD system are important to understanding and predicting atmospheric

variables. In our work, we have found that KAKQ is off by a factor of two when predicting rainfall variation in the Hampton Roads Area. Pairing PAR systems inside a NEXRAD field of view will greatly increase our ability to understand how these motions affect the overall storm and predict the surface effects of these storms. We would be remiss if we did not credit the vast spatial coverage of the NEXRAD system and the work that it supports.
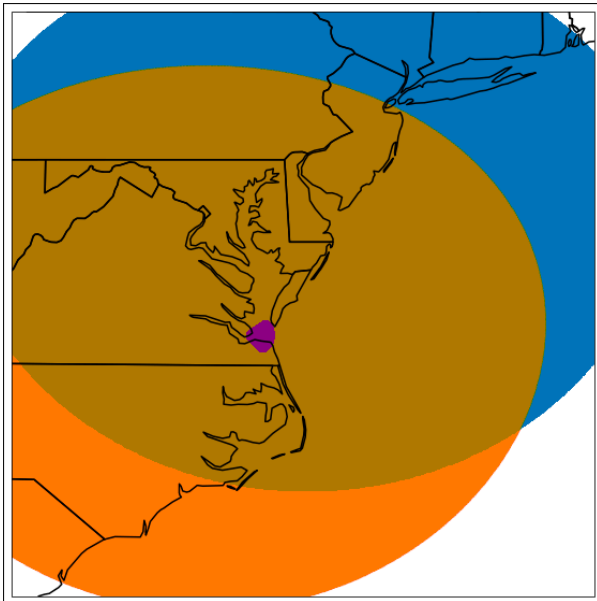
Figure 7. Observational range of NEXRAD KAKQ (*orange*), NEXRAD KDOX (*blue*), and Skyler (*purple*).

PARs are not something that can replace NEXRAD, as the spatial coverage of a PAR is dwarfed by that of NEXRAD, but instrumentation that can be used in conjunction with NEXRAD to help increase our understanding of turbulent motions and help forecast extreme weather events, such as rapid intensification of storms.

We would like to note that for the Hampton Roads Area, forecasting capabilities are limited due to the orientation of Skyler. Most systems here move from West to East, so by the time Skyler can observe a system, it has already passed out into the Chesapeake Bay. However, we indicated that small-scale features are present below KAKQ resolvability, and these can play a large role in the future propagation and damage caused by storms moving through Hampton Roads.

Another object of note is the lack of work we have done with the Radar Radial Velocity. We are searching for a way to accurately resolve a 3D wind field, but the current orientation of KAKQ and Skyler makes full wind retrieval impossible. KAKQ is located nearly along the same latitude line, so both instruments have the same looking angle on atmospheric features. Thus, they have the same looking angle on atmospheric phenomena, which is poor for resolving a 3D wind field. Different looking angles are necessary for this computation, and we currently do not have the instrumentation to compute this.

In the future, we hope to be able to connect the high spatial resolution of the work we are doing here to NASA missions, including the proposed INCUS mission (6), which will measure convective motions through imaging cloud tops on time scales similar to the capability of Skyler. Following the work done to motivate the INCUS plan (11, 12, and 13), we plan to use Skyler in conjunction with INCUS measurements.

CONCLUSION

Skyler can observe and highlight features at scales of 1 km and smaller that the current NWS system is blind to. Understanding how these features are created and the effects they have on the storm system as a whole is important for the forecasting and science communities. Being able to observe our atmosphere at higher spatial and temporal

scales brings these features to light so we can observe, understand, and catalogue them.

APPENDIX

For us to accurately complete the science done above, we first sought to ensure that the radar reflectivity echoes recorded by Skyler were true representations of the storm systems it was viewing. We acknowledge that this bias computation is likely to be imperfect due to the differences in the instrument parameters (such as operational wavelength and gate spacing), viewing parameters (viewing angle, viewing distance, and pulse volume). Skyler, an X-band radar, can also suffer from attenuation effects much sooner than KAKQ, an S-band radar. Also, due to the difference in viewing parameters, matching up identical pulse volumes between the two instruments is difficult, if possible.

To complete this calibration, we have used locally stored data collected from Skyler and pulled past KAKQ data from the online Amazon Warehouse Server (AWS), covering rain events from March 13th, 2023, to January 11th, 2025. During this time, we have data from squall lines, near uniform rain, and other precipitative patterns over the Hampton Roads Area. For our science above, we focused on two specific days, June 23rd, 2023, and November 15th, 2024, but we have used all the data available to us to find a calibration value between the systems. The method for obtaining our calibration is as follows:

1) We first looked through the days that Skyler was operational and selected times that a volume scan contained reflectivity data in at least 28% of its returns. We chose our threshold based on the percent coverage during the passing of a squall line on June 23rd, 2023. This percentage check is done to ensure that the times we are comparing Skyler and KAKQ relate to rain events and not system noise or airborne vehicles.

2) With the day and time of our Skyler files known, we then searched the NEXRAD on AWS database to find KAKQ data files that coincide with the Skyler data files. Since Skyler reports volume scans in $1/10^{th}$ the time it takes KAKQ to report one, we have elected to use the middle time of the KAKQ file for this matching. This middle time is found from the KAKQ file, and then a Skyler volume scan that is also centered on that time is constructed using the locally stored data.

3) Once the two data files have been paired, we use a python script, with the assistance of the pyART module (10), to interact with the datasets in the two files and put them into the same coordinate system. For our purposes, we convert the positional data in both files, which is presented in radar-centered spherical coordinates, into Latitude, Longitude, and altitude, and then into meters East, West, and altitude centered on the Skyler system. Part of this interaction includes using the SNR of the Skyler system to ensure that we are using returns that correspond to real rain events. We found that setting points that have an SNR below 0 to nan helped clean out the noise in both the radar reflectivity and Doppler velocity returns. At this time we also crop the KAKQ dataset to a box around the Skyler field of view, defined as follows: 1 km West to 33 km East of Skyler   26 km South to 22 km North of Skyler Surface to 16 km Altitude. This box is: 34 km x 48 km x 16 km (E/W, N/S, Alt)

4) Once the files are in the same coordinate system, we interpolate both to the same fixed grid, collecting data every 100 m in the E/W and N/S directions and every 250 m in altitude. This allows us to collocate the values from the two radar systems, allowing

us to accurately compare their reflectivity returns at the same position. This interpolation is done in Z units, as opposed to the units where radar reflectivity is reported, dBz. This is to ensure that we are linearly interpolating linear data, not exponential data.

5) Finally, we compute the mean difference between interpolated KAKQ and smoothed and interpolated Skyler reflectivity returns. Computing the mean difference and standard deviation gives a bias of 7.071 ± 3.51 dBz. This value is calculated from our total of 632 individual matchups, covering 17 days. However, in the box and whisker plots shown below, we have elected to generate boxplots for days that have at least 10 files present, leaving us with 546 matchups over 14 days.
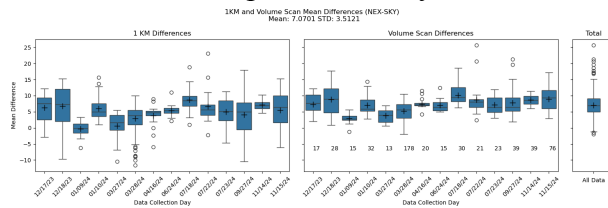
Figure 8. The boxplots shown represent mean difference results. The black plus symbols in each box plot indicate the mean value, while the horizontal black lines indicate the median. Whiskers for each plot cover the 1.5 IQR space, and values beyond that are labeled with open circles and are considered outliers. The values in the middle plot below the boxplots indicate the number of matchups found on that day.

REFERENCES

(1) US Department of Commerce, N (USDC). (2017, July 31). Radar. National Weather Service. https://www.weather.gov/about/radar

(2) American Meteorological Society (AMS). (2024, March 29). WSR–88D. WSR-88D. https://glossary.ametsoc.org/wiki/Wsr-88d

(3) NEXRAD and TDWR Radar Locations and Coverage. Radar Operations Center. (2024, November 1). https://www.roc.noaa.gov/branches/program-branch/site-id-database/site-id-location-maps.php

(4) P. Kollias, D. J. McLaughlin, S. Frasier, M. Oue, E. Luke and A. Sneddon, "Advances and applications in low-power phased array X-band weather radars," 2018 IEEE Radar Conference (RadarConf18), Oklahoma City, OK, USA, 2018, pp. 1359-1364, doi: 10.1109/RADAR.2018.8378762.

(5) P. Kollias, E. P. Luke, K. Tuftedal, M. Dubois and E. J. Knapp, "Agile Weather Observations using a Dual-Polarization X-band Phased Array Radar," 2022 IEEE Radar Conference (RadarConf22), New York City, NY, USA, 2022, pp. 1-6, doi: 10.1109/RadarConf2248738.2022.9764308.

(6) Ward, K., & Bolles, D. (2025, February 27). Incus - NASA Science. NASA. https://science.nasa.gov/mission/incus/

(7) P. R. Drake, J. Bourgeois, A. P. Hopf, F. Lok and D. McLaughlin, "Dual-polarization X-band phased array weather radar: Technology update," 2014 International Radar Conference, Lille, France, 2014, pp. 1-6, doi: 10.1109/RADAR.2014.7060423.

(8) W. Heberling and S. J. Frasier, "On the Projection of Polarimetric Variables Observed by a Planar Phased-Array Radar at X-Band," in IEEE Transactions on Geoscience and Remote Sensing, vol. 59, no. 5, pp. 3891-3903, May 2021, doi: 10.1109/TGRS.2020.3023640.

(9) US Department of Commerce, N. (2018, August 14). Reflectivity-rainfall rate relationships in operational meteorology. National Weather Service. https://www.weather.gov/tae/research-zrpaper

(10) Wang, J., & Wolff, D. B. (n.d.). Wallops precipitation science research facility. NASA. https://wallops-prf.gsfc.nasa.gov/index.php

(11) Helmus, J.J. & Collis, S.M., (2016). The Python ARM Radar Toolkit (Py-ART), a Library for Working with Weather Radar Data in the Python Programming Language. Journal of Open Research Software. 4(1), p.e25. DOI: http://doi.org/10.5334/jors.119

(12) Z. S. Haddad, O. O. Sy, S. Hristova-Veleva and G. L. Stephens, "Derived Observations From Frequently Sampled Microwave Measurements of Precipitation—Part I: Relations to Atmospheric Thermodynamics," in IEEE Transactions on Geoscience and Remote Sensing, vol. 55, no. 6, pp. 3441-3453, June 2017, doi: 10.1109/TGRS.2017.2671598.

(13) O. O. Sy, Z. S. Haddad, G. L. Stephens and S. Hristova-Veleva, "Derived Observations From Frequently Sampled Microwave Measurements of Precipitation. Part II: Sensitivity to Atmospheric Variables and Instrument Parameters," in IEEE Transactions on Geoscience and Remote Sensing, vol. 55, no. 5, pp. 2898-2912, May 2017, doi: 10.1109/TGRS.2017.2656061.

(14) S. Prasanth, Z. S. Haddad, O. O. Sy and R. C. Sawaya, "Derived Observations From Frequently Sampled Microwave Measurements of Precipitation—Part III: Convoys of mm-Wave Radiometers," in IEEE Transactions on Geoscience and Remote Sensing, vol. 60, pp. 1-8, 2022, Art no. 4109608, doi: 10.1109/TGRS.2022.3200863.

(15) Lamer, K., Oue, M., Battaglia, A., Roy, R. J., Cooper, K. B., Dhillon, R., and Kollias, P.: Multifrequency radar observations of clouds and precipitation including the G-band, Atmos. Meas. Tech., 14, 3615–3629, https://doi.org/10.5194/amt-14-3615-2021, 2021.

Mackey